Article

Not peer-reviewed version

Anatomical Barriers to Impregnation in Hybrid Poplar: A Comparative Study of Pit Characteristics in Normal and Tension Wood

Andreas Buschalsky , Holger Militz * , Tim Koddenberg

Posted Date: 20 June 2025

doi: 10.20944/preprints202506.1689.v1

Keywords: poplar; wood anatomy; tension wood; pit characteristics; impreganation

Preprints.org (www.preprints.org) | NOT PEER-REVIEWED | Posted: 20 June 2025 doi:10.20944/preprints202506.1689.v1

Article

Anatomical Barriers to Impregnation in Hybrid Poplar: A Comparative Study of Pit Characteristics in Normal and Tension Wood

Andreas Buschalsky, Holger Militz * and Tim Koddenberg

Faculty of Forest Sciences and Forest Ecology, Wood Biology and Wood Products, University of Göttingen, Büsgenweg 4, 37077 Göttingen, Germany

* Correspondence: holger.militz@uni-goettingen.de

Abstract

Fast-growing hardwoods like poplar often lack natural durability in outdoor use and require homogeneous impregnation with protective agents, though achieving homogeneity remains a known challenge. Various anatomical structures influence fluid transport in wood. This study compares pit characteristics in normal wood and tension wood of a hybrid poplar genotype, including both impregnated (with an aqueos, dye-containing solution) and non-impregnated regions, to identify anatomical barriers to impregnation. Light and scanning electron microscopy revealed significant differences in pit morphology and frequency in libriform fibres between normal wood and tension wood. In non-impregnated regions, pits were often encrusted. Cross-field pits did not differ between normal wood and tension wood but showed distinct differences between impregnated and non-impregnated regions: in the latter, pits were occluded by tylose-forming layers. Intervessel pits differed in border and aperture size between earlywood and latewood in both normal wood and tension wood. Hence, fluid transport is strongly impeded by occluded cross-field pits and, to a lesser extent, by encrusted fibre pits.

Keywords: poplar; wood anatomy; tension wood; pit characteristics; impreganation

---

1. Introduction

In the context of both economic and scientific interests, the group of fast-growing agroforestry hardwood species is gaining increasing relevance. However, in practical outdoor applications, these hardwoods typically exhibit low resistance to biological degradation [1,2]. Therefore, deep and homogeneous impregnation with wood preservatives or wood modification agents is a fundamental requirement for ensuring the durability of these materials [3,4]. In many hardwood species, such as poplar, insufficient and heterogeneous penetration and distribution of impregnation agents within the wood matrix are frequently observed (Figure 1). The cause of this phenomenon has not yet been fully identified, although it is suspected to be related to the microscopic structure of poplar wood. Key structural elements that influence fluid transport include the lumen diameter of vessels, fibres, and parenchyma cells, the frequency of individual cell types, as well as the number and size of pits [5–8]. In addition, the formation of tyloses within the vessels of hardwoods can significantly reduce the natural permeability of the wood by obstructing the longitudinal pathways for fluid movement [9–11].

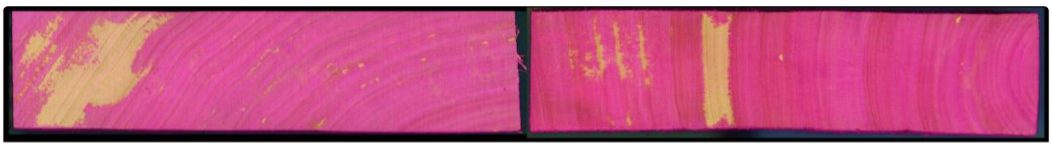

Preprints.org (www.preprints.org) | NOT PEER-REVIEWED | Posted: 20 June 2025 doi:10.20944/preprints202506.1689.v1

Figure 1. Representative images illustrating heterogeneous distribution patterns in poplar wood impregnated with an aqueous, dye-containing solution [12].

Another potential factor that has so far been insufficiently investigated could be reaction wood. Tension wood (TW), as a type of reaction wood only occurring in hardwoods, is frequently observed in fast-growing hardwood species [13]. TW is characterised by the thickening of fibre walls through the formation of a gelatinous layer (G-layer), predominantly composed of cellulose [14,15]. In TW, the microfibrils are almost entirely oriented in a longitudinal direction, parallel to the fibre axis [16]. Recent studies by Buschalsky et al. [12,17] found a significant presence of TW areas in *Populus* × *canadensis*, but their influence on impregnability could not be conclusively determined. Investigations on beech wood (*Fagus sylvatica* L.) revealed that the radial air permeability of TW is reduced in comparison to normal wood (NW). This reduced permeability is assumed to be caused by a lower number and smaller diameter of intervessel pits [18,19]. The primary function of pits is to enable fluid transport between wood cells [20].

This study aims to compare pit characteristics (number, dimensions, and morphology) between TW and NW in a hybrid poplar genotype. Both impregnated and non-impregnated regions are included to enable a comprehensive comparative analysis. The investigation considers multiple cell types, including ray–vessel interfaces (cross-field pits), vessel-to-vessel connections (intervessel pits), and libriform fibres. The primary objective is to identify anatomical differences between TW and NW that may affect fluid transport.

2. Materials and Methods

For the investigations, air-dried boards of poplar wood (*Populus* × *canadensis*, 'Gelrica', Moench) were impregnated after reaching treatability (moisture content < 20%) with a dye-containing aqueous solution (0.05% rhodamine B) using a 2-hour vacuum followed by 5 hours of pressure at 1 MPa. A comprehensive description of the wood material can be found in the study by Buschalsky et al. [17]. The light red hue of rhodamine B allows for macroscopic and microscopic visualisation of the distribution of the absorbed impregnation solution within the wood. This allows both impregnated and non-impregnated regions to be identified.

For microscopic analysis, TW and NW areas were extracted from the boards. The extensive presence of TW was macroscopically identifiable based on the woolly surface texture of the test specimens (Figure 2a,b). From both areas, specimens (n = 5) were prepared with dimensions of 20 (ax.) × 10 × 10 mm^3 from impregnated and non-impregnated areas, respectively. After 24-hour water storage, cross-sectional thin sections (n = 5; 15 µm) were prepared using a sliding microtome from every specimen. For each thin section, 10 grids were evaluated in both earlywood (EW) and latewood (LW) (Figure 3). To differentiate between TW and NW, the thin sections were stained with safranin and astrablue according to Gerlach (1984). Safranin stains the lignin in lignified cell walls red, while astrablue stains cellulose blue. Prior to staining, the sections were decolorised by immersion in 70% ethanol to remove residual rhodamine B. This step ensured that only areas predominantly composed of TW or NW were selected for the subsequent pit analysis. Figure 2c shows an exemplary NW region of a test specimen, while Figure 2d depicts a TW region.

For the examination of pit characteristics, radial specimens encompassing entire annual rings, including both upper and lower ring boundaries, were prepared. This allowed for a comparative assessment of EW and LW regions in both NW and TW. The specimens were examined using a transmitted light microscope (TLM) of the type BZ-X810 (Keyence Deutschland GmbH, Neu-Isenburg, Germany) as well as a scanning electron microscope (SEM) of the type EVO LS 15 (Carl Zeiss Microscopy GmbH, Oberkochen, Germany). The following subsections describe the methodlogies applied for the different cell types.

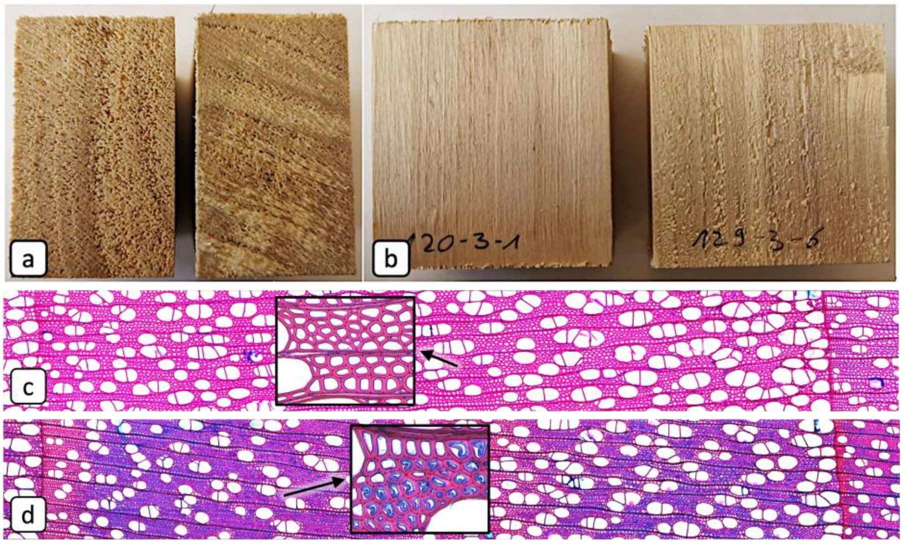

Figure 2. Overview of specimen selection. (a+b) Comparison of specimens with a smooth surface (left) and a "woolly" surface (right). The woolly surface serves as a macroscopic indicator for tension wood (TW). (c) Light microscopic image of an annual ring from an area of normal wood (NW). (d) Light microscopic image of an annual ring from an area of tension wood (TW). Safranin stains the lignin in lignified cell walls red, while astrablue stains cellulose blue. Since the distinctive G-layer of TW consists primarily of cellulose, TW areas can be identified by their blue staining, whereas NW areas appear red.

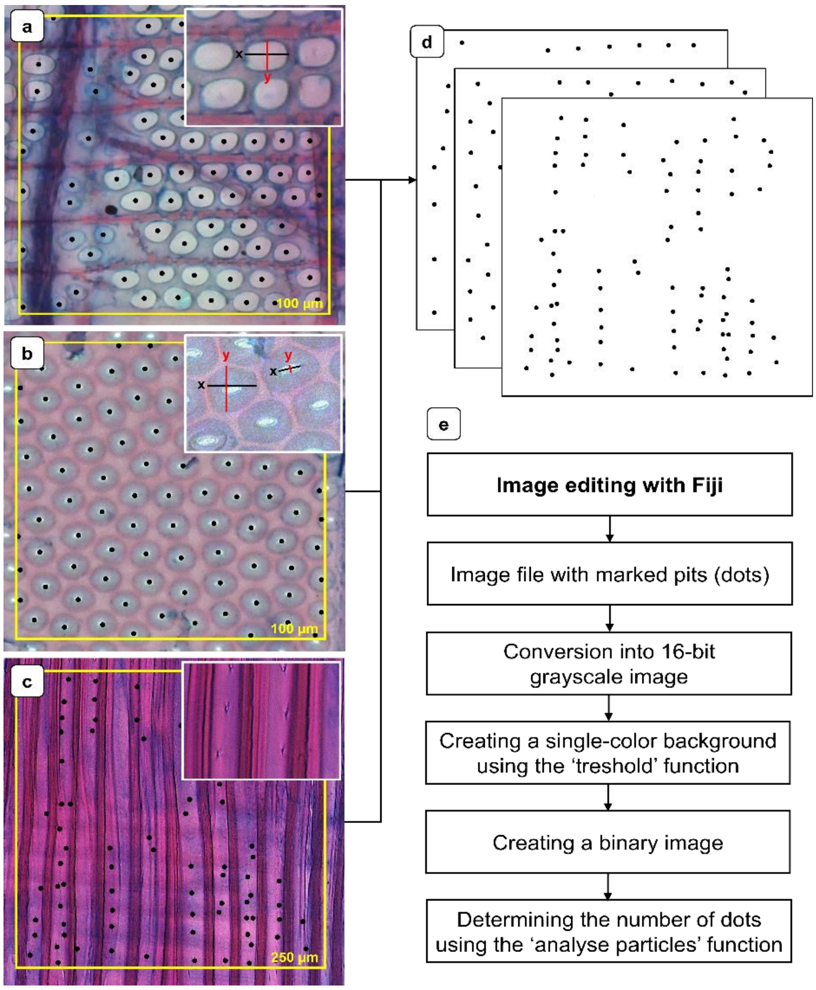

Figure 3. Methodology for assessing pit frequency and dimensions using representative light microscopy images. (a) Radial section showing pitting at the interface between a ray cell and a vessel (cross-field pits). (b)

Preprints.org (www.preprints.org) | NOT PEER-REVIEWED | Posted: 20 June 2025 doi:10.20944/preprints202506.1689.v1

Radial section showing intervessel pitting. (c) Radial section showing pits of libriform fibres. (d) Representative binary images for determining the pit frequency. (e) Flowchart of the image editing procedure.

2.1. Cross-Field Pits and Intervessel Pits

Pit frequency [n 100 µm^{-2}] was assessed on safranin/astrablue-stained radial thin sections (15 µm) using the TLM equipped with a 40× objective lens. Representative images of cross-field pits and intervessel pits are presented in Figure 3a and Figure 3b, respectively. To facilitate quantification, a 100 µm × 100 µm square grid was overlaid on the micrographs, and all pits within the defined area were manually marked using the microscope software (black dots). The resulting images were exported in TIFF format and further processed to binary images (Figure 3d) and subsequently analysed with Fiji image analysis software [21]. The image processing is shown schematically in (Figure 3e).

Pit dimensions were determined using the TLM at 100× objective magnification by performing orthogonal measurements (x and y) of pit length and width (see magnified sections in Figure 3a,b). For intervessel pitting, both the pit apertures and the surrounding pit borders were measured.

2.2. Pits of Libriform Fibres

The determination of pit frequency in libriform fibres [n 250 µm^{-2}] was carried out according to the methodology described above for cross-field and intervessel pits (Figure 3c). Although fibre pits could be identified using TLM, their dimensions were difficult to measure reliably, necessitating analysis via SEM. For this purpose, samples from NW and TW regions were mounted on aluminium stubs (Plano GmbH, Wetzlar, Germany). Subsequently, the stubs were placed in a sputter coater of the type SC7620 (Quantum Design GmbH, Darmstadt, Germany) and made electrically conductive by coating with gold/palladium for 120 s at a plasma current of 18 mA. This coating time resulted in an approximate layer thickness of 10 nm. Focused electron images of the investigated sample areas were generated and saved using the following SEM parameters: accelerating voltage = 3-6 kV; probe current = 10-150 pA; working distance = 2.5-10 mm; OptiBeam Mode = Depth.

2.3. Statistics

A one way analysis of variance (ANOVA) was conducted to identify significant differences in pit frequency and pit dimensions (significance level α = 0.05) among the different cell types, considering EW and LW of both NW and TW. For pit dimensions, x- and y-values were analysed separately and compared independently.

3. Results and Discussion

3.1. Cross-Field Pits

The frequency of cross-field pits was quantified by comparing NW and TW, with further differentiation between EW and LW (Figure 4a). While the mean frequency for NW (EW: 71 ± 11; LW: 69 ± 12) is slightly higher compared to TW (EW: 67 ± 13; LW: 67 ± 12), the difference was not statistically significant. Similarly, no significant differences in mean pit dimensions NW (EW: x = (8,8 ± 0,9) µm, y = (7,0 ± 0,9) µm; LW: x = (8,7 ± 0,9) µm, y = (6,8 ± 0,7) µm) and TW (EW: x = (8,8 ± 0,9) µm, y = (7,0 ± 0,9) µm; LW: x = (8,7 ± 0,9) µm, y = (6,8 ± 0,7) µm) were observed (Figure 4b). These results align with those of Emaminasab et al. [22], who also reported no significant differences in cross-field pit frequency or dimensions between NW and TW in poplar wood. Accordingly, for these two parameters, no impact on wood impregnability could be inferred.

However, the comparative examination of pits in impregnated and non-impregnated regions revealed distinct differences. In impregnated regions, the pits appeared freely permeable, as they were not occluded. This can be seen in both the TLM (Figure 5a,b) and the SEM (Figure 5g,h) images. In contrast, the apertures of pits in non-impregnated regions are occluded. Blue staining of these occlusions with astrablue indicated that they are composed of a cellulose-based substance (Figure

5c,d). Figure 5e shows occluded cross-field pits and a blue-stained structure identified as a tylose. Figure 5f supports this interpretation by presenting tyloses within vessels in cross-section. These structures are also composed of cellulose, as indicated by the staining. The SEM images in Figure 5i,j further illustrate that almost all pits are occluded. Residues of tylosis structures are also visible in these images (yellow arrows). The mechanism of tylosis formation was comprehensively described in the review paper by De Micco et al. [23]. Tyloses are predominantly formed in parenchyma cells of wood rays that are adjacent to a vessel. From these contact cells, a special cell wall layer develops, which extends over the portions of the cell wall that are in contact with the vessel [24–27]. This so-called 'protective layer' or 'tylose-forming layer' is primarily composed of pecto-cellulose [25] and serves as a physical barrier against the swelling of parenchyma cells [26].

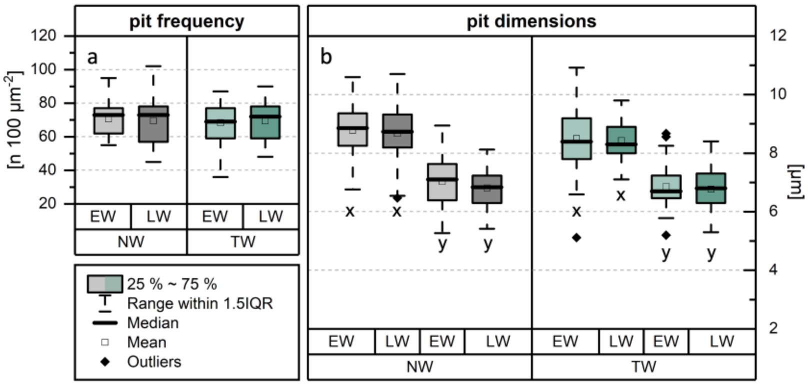

Figure 4. Results of the investigation of pit characteristics within the contact areas between wood rays and vessels (cross-field pits). (a) Comparison of pit frequency between normal wood (NW) and tension wood (TW). (b) Comparison of pit dimensions between NW and TW. The methodology for determining the x- and y-dimensions is shown in Figure 3a.

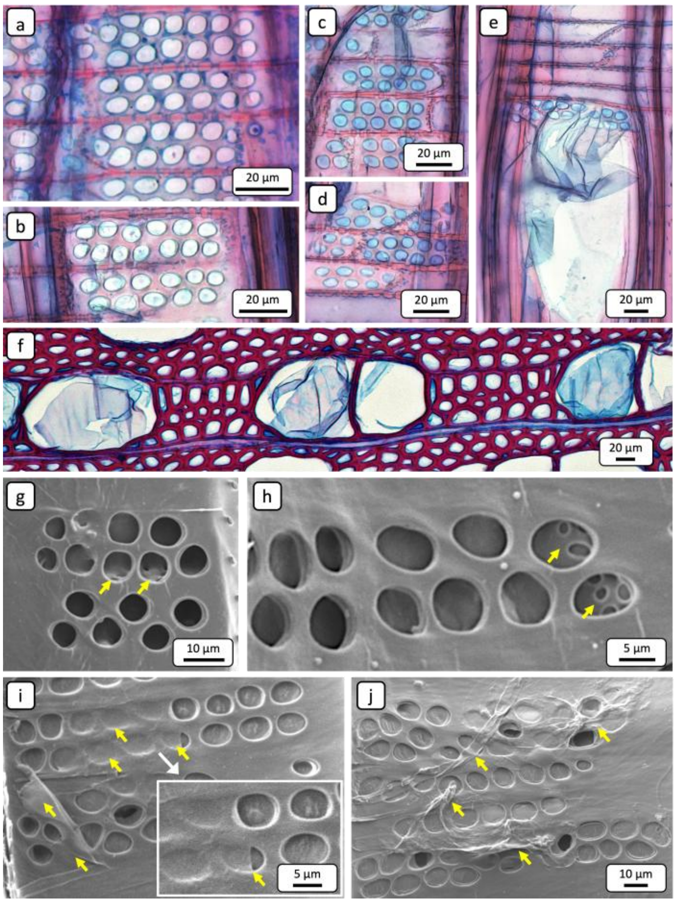

Preprints.org (www.preprints.org) | NOT PEER-REVIEWED | Posted: 20 June 2025 doi:10.20944/preprints202506.1689.v1

Figure 5. Representative TLM (a-f) and SEM (g-j) images for characterising cross-field pits. (a,b) Radial section showing non-occluded pits of an impregnated area. (c,d) Radial section showing occluded pits of a non-impregnated area. The astrablue staining clearly indicates that the occlusion consists of a cellulose-based substance. (e) Radial section showing occluded pits of a non-impregnated area. A tylose is visible, which is also composed of cellulose. (f) Cross-sectional image demonstrating that the blue-stained tyloses are composed of cellulose. (g,h) Radial section showing non-occluded pits of an impregnated area. Through the pit apertures, inter-ray pits are visible (yellow arrows). (i,j) Radial section showing predominantly occluded pits in a non-impregnated area. The pits are partially covered by residues of tylosis material (yellow arrows).

Once the hydrostatic pressure exceeds a critical threshold and the cell wall layer can no longer resist the osmotic pressure of the parenchyma cells, it bulges through the vessel–ray pits into the vessel lumen, resulting in the formation of tyloses [26,28]. A recent study demonstrated that the proportion of tyloses was significantly higher in non-impregnated regions compared to impregnated ones [17]. The pecto-cellulosic composition of the protective layer is consistent with the staining of the pit occlusions with astrablue. Given the high prevalence of tyloses, it can be assumed that the occluded cross-field pits in the non-impregnated regions constitute the physical barrier formed by the protective layer.

In the radial direction, the parenchyma cells of the wood rays are generally considered to play a major role in fluid transport [5,8]. However, these pathways are interrupted by the end walls of the parenchyma cells, which are further characterised by small inter-ray pits (Figure 5g,h; yellow arrows) [29,30]. In poplar, the predominantly uniseriate wood rays are connected to adjacent vessels via large cross-field pits (Figure 5). Consequently, it is more likely that fluids are redirected into adjacent vessels over short distances through ray cells rather than being transported through the entire wood ray. [22]. If the vessels in non-impregnated regions are occluded by tyloses and, in addition, the cross-field pits are blocked by the protective layer, the redirection of fluid flow through the wood rays to adjacent vessels is no longer possible.

3.2. Intervessel Pits

The frequency of intervessel pits was quantified by comparing NW and TW, with further differentiation between EW and LW (Figure 6a). The mean pit frequencies for NW (EW: 56 ± 12; LW: 54 ± 9) and TW (EW: 56 ± 8; LW: 55 ± 11) are comparable, and no statistically significant variations were identified. Comparing the dimensions of the pit borders (Figure 6b), differences between NW and TW were observed in x- and y-dimensions, respectively. Pit borders in TW were smaller in both directions, for both EW (x = (10,1 ± 0,8) µm, y = (8,9 ± 0,7) µm) and LW (x = (8,7 ± 1,1) µm, y = (8,2 ± 0,8) µm) compared to NW (EW: x = (10,9 ± 1,2) µm, y = (9,0 ± 0,9) µm; LW: x = (9,9 ± 1,2) µm, y = (8,7 ± 0,8) µm). Although the differences were relatively small, they were statistically significant according to the ANOVA. Comparing the dimensions of the pit apertures between NW and TW (Figure 6c), statistically significant differences were found only in the x-dimensions within EW. These findings contrast with those reported for *Populus nigra* [22], where no significant differences in average intervessel pit diameter were observed. However, the results regarding pit frequency are consistent. Studies on *Fagus sylvatica* [19,31] showed that the intervessel pits in TW are significantly smaller compared to NW. Nevertheless, the differences reported in the cited studies were substantially greater than those observed in the present investigation.

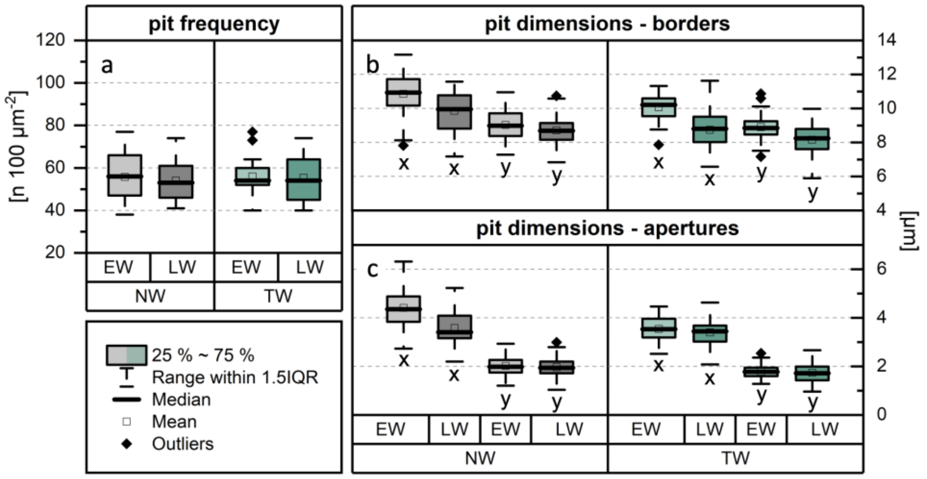

Figure 6. Results of the analysis of intervessel pit characteristics. (a) Comparison of pit frequency between normal wood and tension wood. (b) Comparison of dimensions of pit borders between normal wood (NW) and tension wood (TW). (c) Comparison of dimensions of pit apertures between NW and TW. The methodology for determining the x- and y-dimensions is shown in Figure 3b.

Moreover, significant differences in both dimensional parameters were observed comparing EW (Figure 7a-c) and LW (Figure 7d). The most pronounced differences occurred in the x-dimensions of the pit borders (Figure 6b) in both NW and TW (see values in the previous paragraph), as well as in the pit apertures (Figure 6c) of NW (EW: x = (4,4 ± 0,8) µm; LW: x = (3,6 ± 0,7) µm). Differences in the size of bordered pits between EW and LW have previously been described for tracheids in softwoods [32]. The present findings confirm that these differences also apply to vessels in *Populus* × *canadensis*. This suggests that the vessels in EW are more permeable than those in LW because intervessel pits are the main pathways for fluid movement between vessel elements. In this context, the structure and frequency of the pits are particularly important [33].

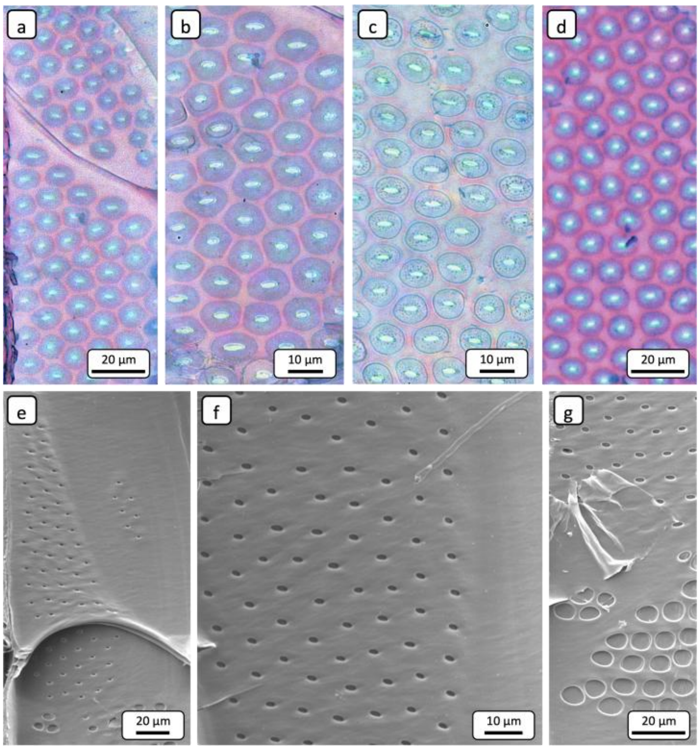

Figure 7. Representative TLM (a-d) and SEM (e-g) images for characterising intervessel pits. (a) Radial section showing bordered pits in earlywood (b) Pits at higher magnification. The focal plane was adjusted to provide a

 doi:10.20944/preprints202506.1689.v1

top-down view of the pit borders. (c) The focal plane is adjusted to allow visualisation of the inner structure of the pit borders. (d) Radial section showing bordered pits in latewood. (e,f) Radial sections showing pits at different magnifications. Pit borders are not visible under the applied SEM imaging parameters. (g) Tylose residue partially covering several of the intervessel pits in a non-impregnated area. Cross-field pits are occluded.

3.3. Pits in Libriform Fibres

The frequency of pits in libriform fibres was quantified by comparing NW and TW, with further differentiation between EW and LW (Figure 8a). The mean frequency in NW (EW: 90 ± 25; LW: 92 ± 29) was significantly higher—approximately twice as high—compared to that observed in TW (EW: 54 ± 15; LW: 46 ± 17).

Regarding pit morphology, TLM (Figure 9a) and SEM (Figure 9c-f) images showed that NW fibres have simple, slit-like pits. In contrast, pits in TW fibres (EW: (16,6 ± 2,8) µm; LW: (17,9 ± 2,6) µm) are significantly more elongated (Figure 9b,i,j), exhibiting a longitudinal expansion more than four times greater than that of pits in NW fibres (EW: (4,0 ± 1,0) µm; LW: (4,6 ± 1,3) µm) (Figure 8b). The significantly greater pit elongation in TW suggests that fewer pits occur per area compared to NW, which provides a plausible explanation for the observed differences in pit frequency.

Furthermore, differences in aperture size were observed (Figure 8c). The results of the orthogonal measurements revealed that the transversal diameter (x-dimensions) of the apertures in NW fibre (EW: (2,4 ± 0,2) µm; LW: (2,4 ± 0,3) µm) pits is significantly larger —approximately twice as high—than that in TW fibre pits (EW: (1,2 ± 0,2) µm; LW: (1,2 ± 0,2) µm). In contrast, the longitudinal diameter (y-dimensions) exhibited only minor differences. Consequently, the pits in NW and TW fibres can be clearly distinguished based on their morphology. For *Populus nigra*, similar descriptions of pronounced morphological differences between the pits of NW and TW fibres have been reported, with the latter being oriented in the direction of the microfibrils [22].

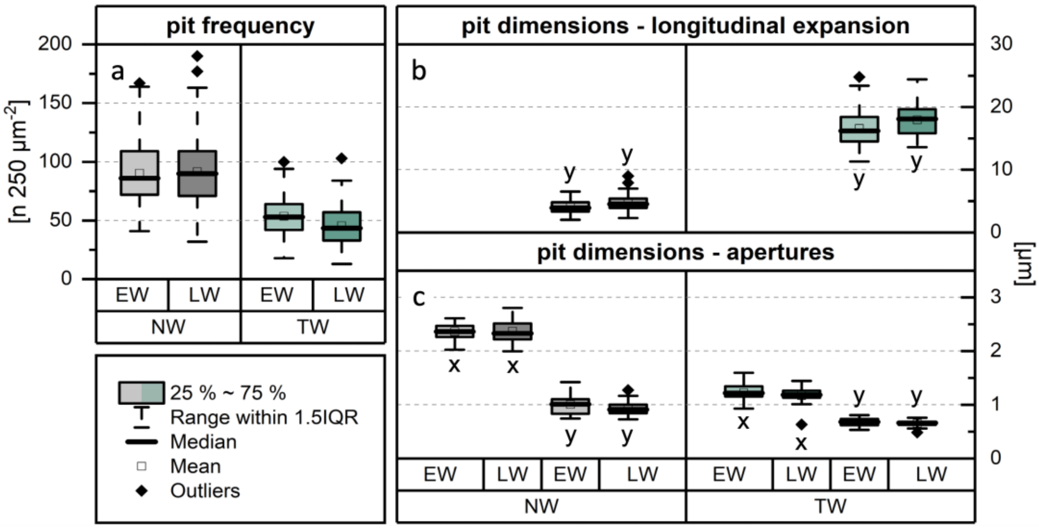

Figure 8. Results of the analysis of pit characteristics in libriform fibres. (a) Comparison of pit frequency between normal wood and tension wood. (b) Comparison of the longitudinal expansion of the pits between normal wood (NW) and tension wood (TW). (c) Comparison of dimensions of pit apertures between NW and TW.

In addition to fibre pits with clearly identifiable apertures, pits lacking a well-defined or even completely absent aperture were also observed in non-impregnated regions, in both NW (Figure 9g,h) and TW (Figure 9k,l). These pits appear to be partially or completely occluded by a substance. Similar observations of pit encrustations have been reported in hardwoods [34,35], including poplar [36]. The exact composition of these encrustations has not yet been conclusively determined. It is evident that encrustation of fibre pits results in a reduction in permeability. However, given the substantially higher permeability of vessels compared to fibres [29], caused by their numerous inter-

Preprints.org (www.preprints.org) | NOT PEER-REVIEWED | Posted: 20 June 2025 doi:10.20944/preprints202506.1689.v1

and intravessel pits, the overall impact of such fibre pit encrustations on total wood permeability is likely to be negligible.

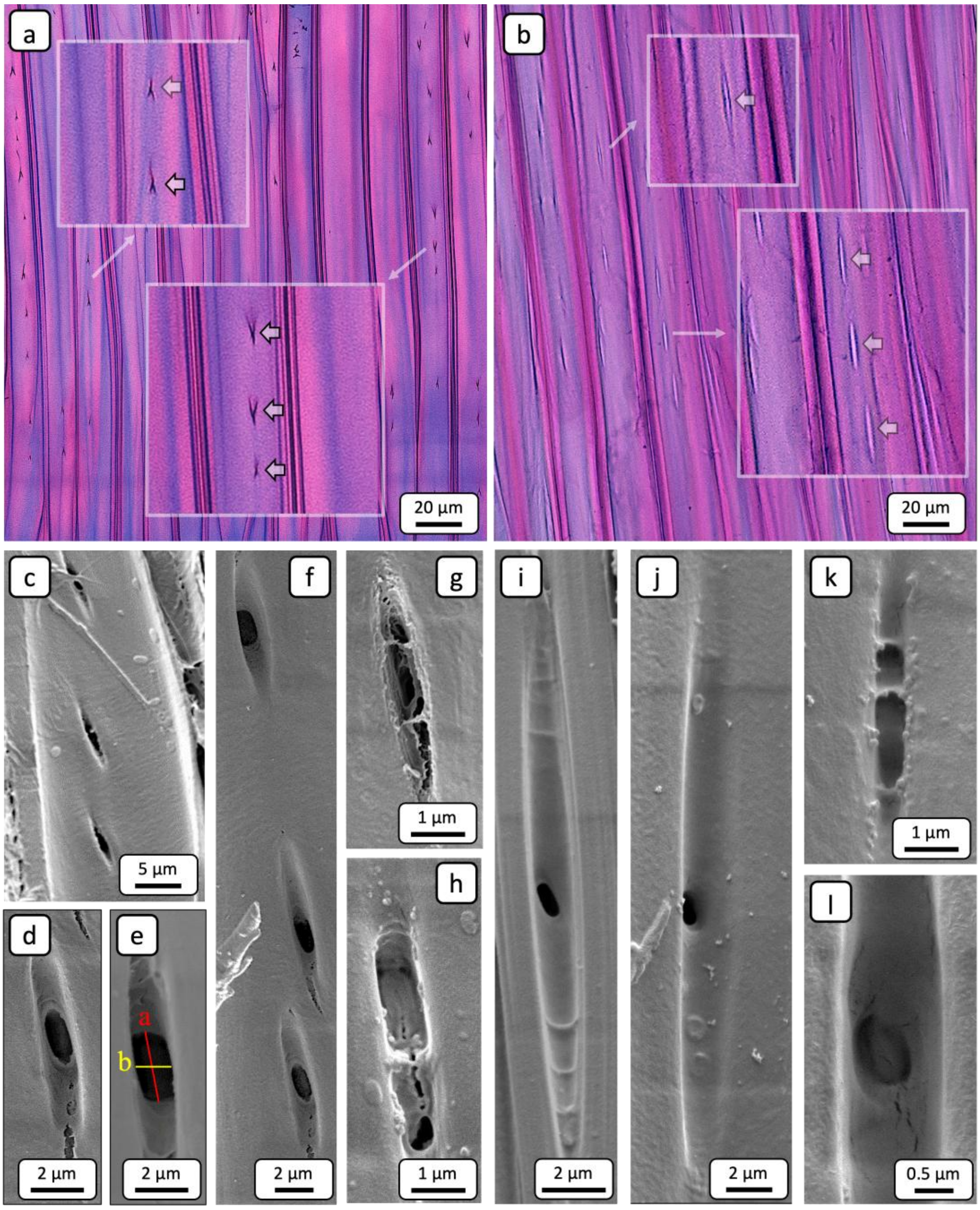

Figure 9. Representative TLM (a,b) and SEM (c-l) images for characterising pits in libriform fibres. (a) Radial section showing pits in normal wood; inset squares provide magnified views. (b) Radial section showing pits in tension wood; inset squares provide magnified views. (c-f) Simple, slit-like pits in normal wood. (g,h) Encrusted pits in normal wood from a non-impregnated area. (i,j) Pits in tension wood that are significantly more elongated compared to those in normal wood. (k,l) Encrusted pits in tension wood from a non-impregnated area.

4. Conclusions

The primary objective of the study was the identification of anatomical differences between tension wood and normal wood that may serve as barrier to impregnation. The most pronounced anatomical differences were observed in the pits of libriform fibres. Fibre pits in tension wood were significantly more elongated, their frequency was lower, and they exhibtited smaller transverse apertures. Furthermore, in non-impregnated regions encrusted fibre pits were observed. However,

 doi:10.20944/preprints202506.1689.v1

the overall impact of both the morphological differences between normal wood and tension wood and the encrustations of fibre pits on total wood permeability is likely to be negligible.

Although no significant differences were found between cross-field pits comparing normal wood and tension wood, pit occlusions of cross-field pits, which are predominantly composed of cellulose-based material, were observed in non-impregnated regions, presenting a distinct physical barrier, strongly impending fluid transport.

Furthermore, anatomical differences were found in intervessel pits. Intervessel pits in tension wood were significantly smaller than those in normal wood. However, since the differences were still minor, their impact on permeability is difficult to assess. A more pronounced difference in pit dimensions was observed when comparing earlywood and latewood within normal wood, suggesting that the vessels in earlywood are more permeable than those in latewood.

Overall, the results indicate that anatomical differences in pit morphology between normal wood and tension wood have only a minor influence on the overall permeability of the wood. In contrast, structural differences between impregnated and non-impregnated areas have a greater impact.

Author Contributions: Conceptualisation, A.B. and T.K.; methodology A.B.; formal analysis, A.B. and T.K.; investigation, A.B.; data curation, A.B.; writing—original draft preparation, A.B.; writing—review and editing, H.M. and T.K.; visualisation, A.B.; project administration, H.M. and T.K.; funding acquisition, H.M. and T.K. All authors have read and agreed to the published version of the manuscript.

Funding: This article was funded by the German Research Foundation (DFG) (grant number: 275616905).

Data Availability Statement: The original contributions presented in this study are included in the article. Further inquiries can be directed to the corresponding author(s).

Acknowledgments: The authors gratefully acknowledge the Dutch timber merchant JF van Boeckel for providing and supplying the test material, as well as Britt Janßen and Caroline Marie Christine Caesar for their practical assistance with the light microscopic investigations. This article is a revised and expanded version of a conference paper entitled 'Vergleich der Tüpfelcharakteristika zwischen Zug- und Normalholz bei Pappel (*Populus × canadensis*, Moench)', which was presented at 6. Holzanatomisches Kolloquium, Dresden, Germany, 7.-8. November 2024.

Conflicts of Interest: The authors declare no conflict of interest.

Abbreviations

The following abbreviations are used in this manuscript:

NW	normal wood
TW	tension wood
EW	earlywood
LW	latewood
TLM	transmitted light microscope
SEM	scanning electron microscope

References

1. Eriksson, K.-E.L.; Blanchette, R.A.; Ander, P. *Microbial and Enzymatic Degradation of Wood and Wood Components*; Springer Series in Wood Science; Springer Berlin Heidelberg: Berlin, Heidelberg, 1990; ISBN 978-3-642-46689-2.
2. *Wood and Tree Fungi: Biology, Damage, Protection, and Use*; Schmidt, O., Ed.; Springer Berlin Heidelberg, 2006; ISBN 978-3-540-32138-5.
3. Tsoumis, G. *Science and Technology of Wood: Structure, Properties, Utilization*; Reprint of the ed. New York 1991.; Kessel: Remagen-Oberwinter, 2009; ISBN 978-3-941300-22-4.

Preprints.org (www.preprints.org) | NOT PEER-REVIEWED | Posted: 20 June 2025 doi:10.20944/preprints202506.1689.v1

4. Van Acker, J.; Van Den Bulcke, J.; Forsthuber, B.; Grüll, G. Wood Preservation and Wood Finishing. In *Springer Handbook of Wood Science and Technology*; Niemz, P., Teischinger, A., Sandberg, D., Eds.; Springer Handbooks; Springer International Publishing: Cham, 2023; pp. 793–871 ISBN 978-3-030-81314-7.
5. Cŏté, W.A. Structural Factors Affecting the Permeability of Wood. *Journal of Polymer Science Part C: Polymer Symposia* **1963**, *2*, 231–242, doi:10.1002/polc.5070020122.
6. Grosser, D. *Die Hölzer Mitteleuropas: Ein mikrophotographischer Lehratlas*; reprint of the original 1st ed. 1977.; Kessel: Remagen, 2007; ISBN 978-3-935638-22-7.
7. Hansmann, C.; Gindl, W.; Wimmer, R.; Teischinger, A. Permeability of Wood - A Review. *Wood Research* **2002**, *47*, 1–16.
8. Thybring, E.E.; Fredriksson, M. Wood and Moisture. In *Springer handbook of wood science and technology*; Niemz, P., Teischinger, A., Sandberg, D., Eds.; Springer Handbooks; Springer International Publishing: Cham, 2023; pp. 355–397 ISBN 978-3-030-81314-7.
9. Wardrop, A.B.; Davies, G.W. Morphological Factors Relating to the Penetration of Liquids into Wood. *Holzforschung* **1961**, *15*, 129–141, doi:10.1515/hfsg.1961.15.5.129.
10. Silva, M.R.; Machado, G.; Deiner, J.; Calil Junior, C. Permeability Measuremens of Brazilian Eucalyptus. *Mat. Res.* **2010**, *13*, 281–286, doi:10.1590/S1516-14392010000300002.
11. Taghiyari, H.R.; Karimi, A.-N.; Parsapajouh, D.; Pourtahmasi, K. Study on the Longitudinal Gas Permeability of Juvenile Wood and Mature Wood. *Special Topics Rev Porous Media* **2010**, *1*, 31–38, doi:10.1615/SpecialTopicsRevPorousMedia.v1.i1.30.
12. Buschalsky, A.; Löning, S.; Militz, H.; Koddenberg, T. Structural Characterisation of the Variable Impregnation of Poplar Wood. In Proceedings of the Hardwood Conference Proceedings; University of Sopron Press: Sopron, Hungary, 14.10 2022; pp. 28–36.
13. Cuenderlik, I.; Kudela, J.; Molinski, W. Reaction Beech Wood in Drying Process.; Vienna, Austria, 1992; pp. 350–353.
14. Ruelle, J. Morphology, Anatomy and Ultrastructure of Reaction Wood. In *The Biology of Reaction Wood*; Gardiner, B., Barnett, J., Saranpää, P., Gril, J., Eds.; Springer Series in Wood Science; Springer Berlin Heidelberg: Berlin, Heidelberg, 2014; pp. 13–35 ISBN 978-3-642-10813-6.
15. Scurfield, G. Reaction Wood: Its Structure and Function: Lignification May Generate the Force Active in Restoring the Trunks of Leaning Trees to the Vertical. *Science* **1973**, *179*, 647–655, doi:10.1126/science.179.4074.647.
16. Du, S.; Yamamoto, F. An Overview of the Biology of Reaction Wood Formation. *J. Integr. Plant Biol.* **2007**, *49*, 131–143, doi:10.1111/j.1744-7909.2007.00427.x.
17. Buschalsky, A.; Löning, S.; Siegel, K.; Militz, H.; Koddenberg, T. Macroscopic and Microscopic Investigations of the Inhomogeneous Distribution of Impregnating Agents in Poplar Wood (*Populus × Canadensis* Moench). *Wood Material Science & Engineering* **2025**, 1–13, doi:10.1080/17480272.2025.2507819.
18. *The Biology of Reaction Wood*; Gardiner, B., Barnett, J., Saranpää, P., Gril, J., Eds.; Springer Series in Wood Science; Springer Berlin Heidelberg: Berlin, Heidelberg, Germany, 2014; ISBN 978-3-642-10813-6.
19. Tarmian, A.; Perré, P. Air Permeability in Longitudinal and Radial Directions of Compression Wood of Picea Abies L. and Tension Wood of Fagus Sylvatica L. *Holzforschung* **2009**, *63*, doi:10.1515/HF.2009.048.
20. Schmitt, U.; Koch, G.; Hietz, P.; Tholen, D. Wood Biology. In *Springer Handbook of Wood Science and Technology*; Niemz, P., Teischinger, A., Sandberg, D., Eds.; Springer Handbooks; Springer International Publishing: Cham, 2023; pp. 41–138 ISBN 978-3-030-81314-7.
21. Schindelin, J.; Arganda-Carreras, I.; Frise, E.; Kaynig, V.; Longair, M.; Pietzsch, T.; Preibisch, S.; Rueden, C.; Saalfeld, S.; Schmid, B.; et al. Fiji: An Open-Source Platform for Biological-Image Analysis. *Nat Methods* **2012**, *9*, 676–682, doi:10.1038/nmeth.2019.
22. Emaminasab, M.; Tarmian, A.; Oladi, R.; Pourtahmasi, K.; Avramidis, S. Fluid Permeability in Poplar Tension and Normal Wood in Relation to Ray and Vessel Properties. *Wood Sci Technol* **2017**, *51*, 261–272, doi:10.1007/s00226-016-0860-y.
23. De Micco, V.; Balzano, A.; Wheeler, E.A.; Baas, P. Tyloses and Gums: A Review of Structure, Function and Occurrence of Vessel Occlusions. *IAWA J* **2016**, *37*, 186–205, doi:10.1163/22941932-20160130.
24. Foster, R.C. Fine Structure of Tyloses. *Nature* **1964**, *204*, 494–495, doi:10.1038/204494a0.

25. Czaninski, Y. Vessel-Associated Cells. *IAWA Bulletin* **1977**, *3*, 51–55.
26. Van Bel, A.J.E.; Van Der Schoot, C. Primary Function of the Protective Layer in Contact Cells: Buffer against Oscillations in Hydrostatic Pressure in the Vessels? *IAWA J* **1988**, *9*, 285–288, doi:10.1163/22941932-90001078.
27. Evert, R.F. *Esau's Plant Anatomy: Meristems, Cells, and Tissues of the Plant Body: Their Structure, Function, and Development*; 1st ed.; Wiley, 2006; ISBN 978-0-471-73843-5.
28. Schaffer, K.; Wisniewski, M. Development of the Amorphous Layer (Protective Layer) in Xylem Parenchyma of Cv. Golden Delicious Apple, Cv. Loring Peach, and Willow. *Amer. J. Bot.* **1989**, *76*, 1569–1582, doi:10.1002/j.1537-2197.1989.tb15142.x.
29. Ahmed, S.A.; Chun, S.K. Observation of Liquid Permeability Related to Anatomical Characteristics in *Samanea Saman*. *Turk J Agric For* **2009**, doi:10.3906/tar-0807-13.
30. Ahmed, S.A.; Chun, S.K. Permeability of *Tectona Grandis* L. as Affected by Wood Structure. *Wood Sci Technol* **2011**, *45*, 487–500, doi:10.1007/s00226-010-0335-5.
31. Tarmian, A.; Remond, R.; Faezipour, M.; Karimi, A.; Perré, P. Reaction Wood Drying Kinetics: Tension Wood in Fagus Sylvatica and Compression Wood in Picea Abies. *Wood Sci Technol* **2009**, *43*, 113–130, doi:10.1007/s00226-008-0230-5.
32. Stamm, A.J. Maximum Effective Pit Pore Radius of the Heartwood and Sapwood of Six Softwoods Affected by Drying and Soaking. *Wood and Fiber* **1970**, *1*, 263–269.
33. Sano, Y. Intervascular Pitting across the Annual Ring Boundary in Betula Platyphylla Var. Japonica and Fraxinus Mandshurica Var. Japonica. *IAWA J* **2004**, *25*, 129–140, doi:10.1163/22941932-90000355.
34. Gale, R. Some Pitfalls in Wood Identification, with Reference to Nothofagus. *IAWA J* **1982**, *3*, 179–184, doi:10.1163/22941932-90000837.
35. Thomas, R.J. Anatomical Features Affecting Liquid Penetrability in Three Hardwood Species. *Wood and Fiber* **1976**, *7*, 256–263.
36. Murphy, R.J.; Din, S.U.; Stone, M.J. Observations on Preservative Penetration in Poplar. In Proceedings of the Proceedings IRG Annual Meeting; Kyoto, Japan, 1991; p. 7 pp. IRG/WP 3662.